Synthesis, Characterization, and Electrochemistry of Heterometallic Dendrimers

Sudhir Achar,[†] Chad E. Immoos,[‡] Michael G. Hill,[‡] and Vincent J. Catalano*[,†]

Department of Chemistry/216, University of Nevada, Reno, Nevada 89557, and
Department of Chemistry, Occidental College, Los Angeles, California 90041

Received November 27, 1996[⊗]

A method for the synthesis of new heterometallic dendritic molecules containing organoplatinum centers is reported. Reaction of $Pt_2Me_4(\mu\text{-}SMe_2)_2$ with bpy-Fc_2 (**1**) (bpy-Fc_2 = 4,4′-bis(ferrocenylvinyl)-2,2′-bipyridine) gave the platinum(II) complex $PtMe_2$(bpy-Fc_2) (**2**). Complex **2** undergoes oxidative addition with iodomethane to yield $PtMe_3I$(bpy-Fc_2) (**3**) and with bis(bromomethyl)benzenes to yield complexes of the type [$PtMe_2Br$(bpy-Fc_2)-CH_2−]$_2$R (**4**, R = 1,2-C_6H_4; **5**, R = 1,3-C_6H_4; **6**, R = 1,4-C_6H_4). **1**, **3**, and **4** were characterized by X-ray structure determinations. For **1**, a = 11.780(3) Å, b = 10.662(3) Å, c = 11.642(3) Å, β = 118.61(2)°, and V = 1283.7(6) Å^3 while, for **2,** a = 11.497(2) Å, b = 22.796(6) Å, c = 15.801(3) Å, β = 106.08(1)°, and V = 3979(2) Å^3. Only poor quality crystals of **4** could be obtained resulting in a partial structure refinement with a = 14.46-(1) Å, b = 15.14(1) Å, c = 21.32(2) Å, α = 69.45(4)°, β = 71.14(5)°, γ = 81.86(5)° and V = 4140(6) Å^3. The preferred conformation for **1** places the the bipyridine groups anti with respect to each other. However, as a consequence of the coordination to the metal centers in **3** and **4,** they are located cis to each other, and the cyclopentadienyl rings attached directly to the vinyl groups lie on the same plane. In compound **4** the planes containing the platinum bipyridine units lie above and below the plane of the benzene ring, presumably to minimize steric hindrance. **2** also reacts with 1,3,5-tris(bromomethyl)mesitylene, 1,2,4,5-tetrakis(bromomethyl)benzene, and 1,2,3,4,5,6-hexakis(bromomethyl)benzene in 3:1, 4:1, and 6:1 molar ratios to yield the dendritic molecules [$PtMe_2Br$(bpy-Fc_2)CH_2−]$_n$R [**7**, n = 3, R = 1,3,5-$C_6(CH_3)_3$; **8**, n = 4, R = 1,2,4,5-C_6H_2; **9**, n = 6, R = 1,2,3,4,5,6-C_6], respectively. The largest dendrimer **9** contains six platinum and 12 ferrocene centers. Each complex undergoes a single 2n-electron electrochemical oxidation (corresponding to the ferrocenium/ferrocene couple of the bpy-Fc_2 ligands), confirming that the pendant ferrocenyl units are noninteracting. The number of ferrocene centers for each complex was determined both by exhaustive electrolysis and by a chronocoulometric/voltammetric assay.

Introduction

Dendritic molecules are branched molecules that can be synthesized by convergent, divergent, or combinational methods.[1] Most reported dendritic molecules are organic materials, but organometallic dendritic molecules have received increasing attention due to their unique properties.[2] Inorganic and organometallic dendritic molecules containing ruthenium,[3] platinum,[4] iron,[5] gold,[6] silicon,[7] cobalt,[8] and nickel[9] have been prepared, and organosilicon dendrimers featuring ferrocenyl[10] or nickel-containing groups[9] have been reported. However, there appear to be no examples of organometallic dendritic molecules that contain different transition metals in different layers.

The characterization of inorganic and organometallic dendritic compounds can be exceedingly difficult. Becasue of their large size, limited mobilities, and poor solubilities, standard methods are not always amenable. For example Fréchet[11] was able to characterize the purely organic benzyloxy benzyl dendrimer, $C_{5585}H_{4860}O_{765}$, using standard techiniques (including ^{1}H and ^{13}C NMR, infrared, mass spectrometry, elemental analysis, and size exclusion chromatography), yet the much smaller 1090 atom polypyridine-based, cationic dendrimer containing 22 ruthenium atoms[12] did not lend itself to simple characterization. This was a consequence of its intrinsic stereochemistry, high charge (44+!), and low solubility.

The inclusion of redox-active centers into dendridic materials offers an alternative method for characterization. For example,

[†] University of Nevada.
[‡] Occidental College.
[⊗] Abstract published in *Advance ACS Abstracts,* April 1, 1997.

(1) (a) Issberner, J.; Moors, R.; Vögtle, F. *Angew. Chem., Int. Ed. Engl.* **1994**, *33*, 2413. (b) Ardoin, N.; Astruc, D. *Bull. Soc. Chim. Fr.* **1995**, *132*, 875. (c) Mekelburger, H. B.; Jaworek, W.; Vögtle, F. *Angew. Chem., Int. Ed. Engl.* **1992**, *31*, 1571. (d) Tomalia, D. A.; Naylor, A. M.; Goddard, W. A. III. *Angew. Chem., Int. Ed. Engl.* **1990**, *29*, 138. (e) Xu, Z. F.; Kahr, M.; Walker, K. L.; Wilkins, C. L.; Moore, J. S. *J. Am. Chem. Soc.* **1994**, *116*, 4537. (f) Newcome, G. R. *Dendritic Molecules: Concepts, Synthesis, Perspective*; VCH: Weinheim, Germany, 1996.
(2) Dagani, R. *Chem. Eng. News* **1996**, 30.
(3) (a) Balzani, V.; Campagna, S.; Denti, G.; Juris, A.; Serroni, S.; Venturi, M. *Coord. Chem. Rev.* **1994**, *132*, 1. (b) Serroni, S.; Denti, G.; Campagna, S.; Juris, A.; Ciano, M.; Balzani, V. *Angew. Chem., Int. Ed. Engl.* **1992**, *31*, 1493. (c) Newkome, G. R.; Cardullo, F.; Constable, E. C.; Moorefield, C. N.; Thompson, A. M. W. C. *J. Chem. Soc., Chem. Commun.* **1993**, 925. (d) Liao, Y. H.; Moss, J. R. *J. Chem. Soc., Chem. Commun.* **1993**, 1774. (e) Constable, E. C.; Haverson, P.; Oberholzer, M. *J. Chem. Soc., Chem. Commun.* **1996**, 1821.
(4) (a) Achar, S.; Vittal, J. J.; Puddephatt, R. J. *Organometallics* **1996**, *15*, 43. (b) Achar, S.; Puddephatt, R. J. *J. Chem. Soc., Chem. Commun.* **1994**, 1895. (c) Achar, S.; Puddephatt, R. J. *Angew. Chem., Int. Ed. Engl.* **1994**, *33*, 847.
(5) (a) Fillaut, J. L.; Astruc, D. *J. Chem. Soc., Chem. Commun.* **1993**, 1320.
(6) Lange, P.; Beruda, H.; Hiller, W.; Schmidbauer, H. *Inorg. Chem.* **1996**, *35*, 637.
(7) (a) Vandermade, A. W.; Vanleeuven, P. W. N. M.; Dewilde, J. C.; Brandes, R. A. C. *Adv. Mater.* **1993**, *5*, 466. (b) Seyferth, D.; Son, D. Y.; Rheingold, A. L.; Ostrander, R. L. *Organometallics* **1994**, *13*, 2682.
(8) Newkome, G. R.; Moorefield, C. N. *Polm. Prepr. Am. Chem. Soc. Div. Polym. Chem.* **1993**, *34*, 75.
(9) Knapen, J. W. J.; van der Made, A. W.; de Wilde, J. C.; van Leeuwen, P. W. N. M.; Wilkens, P.; Grove, D. M.; van Koten, G. *Nature* **1994**, *372*, 659.
(10) Alonso, B.; Guadrado, I.; Morán, M.; Losada, J. *J. Chem. Soc., Chem. Commun.* **1994**, 2575.
(11) Wooley, K. L.; Hawker, C. J.; Fréchet, J. M. *J. Am. Chem. Soc.* **1991**, *113*, 4252.
(12) Serroni, S.; Denti, G.; Campagna, S.; Juris, A.; Ciano, M.; Balzani, V. *Angew. Chem., Int. Ed. Engl.* **1992**, *31*, 1493.
(13) Moulines, F.; Djakovitch, L.; Boese, R.; Gloaguen, B.; Thiel, W.; Fillaut, J.-l.; Delville, M.-H.; Astruc, D. *Angew. Chem., Int. Ed. Engl.* **1993**, *32*, 1075.

S0020-1669(96)01435-8 CCC: $14.00

Scheme 1

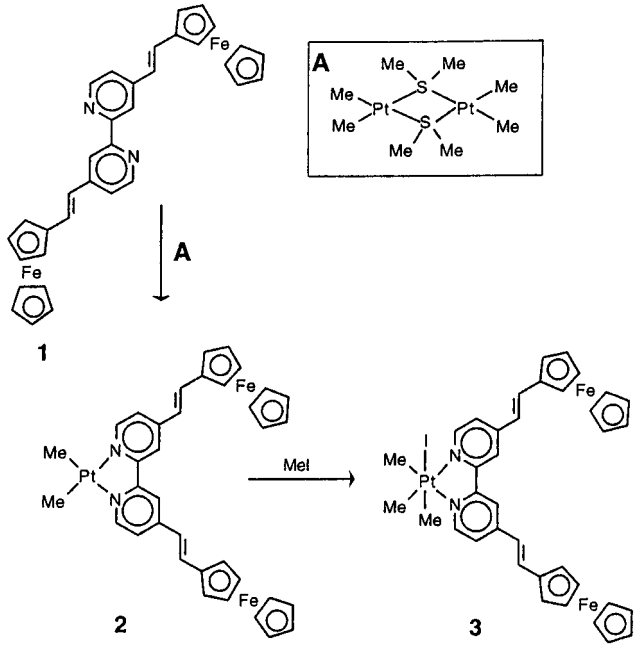

a treelike molecule containing nine equivalent ferrocene units was reported[13] to undergo a single, reversible nine-electron electrochemical oxidation distinguishing this species from other ferrocene-containing moieties. Herein, we report the convergent synthesis of the first examples of heterometallic dendritic molecules. These compounds feature platinum(IV) units arranged in a concentric fashion around a central organic moiety, with ferrocenyl groups directed towards the periphery of the molecule. In addition to X-ray crystallography, NMR spectroscopy, and elemental analysis, the composition of these materials has been determined by a simple electrochemical assay. This assay may prove useful as a characterization tool for other redox containing dendritic molecules.

Results and Discussion

Our key reagent in this work, the α-diimine bpy-Fc_2, **1**, was synthesized by dilithiation of 4,4′-dimethyl-2,2′-bipyridine with lithium diisopropylamide, followed by reaction with ferrocene carboxaldehyde and subsequent dehydration in presence of pyridinium toluene-*p*-sulfonate.[14] Treatment of $[Pt_2Me_4(\mu\text{-}SMe_2)_2]$ with compound **1** yielded the heterometallic trinuclear complex $[PtMe_2(bpy\text{-}Fc_2)]$, **2**, in high yield (Scheme 1). This complex was isolated as an air-stable burgundy solid. The ^{1}H NMR spectrum of **2** features a singlet in the ^{1}H NMR spectrum (due to the two equivalent methyl groups) with a platinum coupling constant of 86 Hz. In addition, the signals due to the ortho protons of the bipyridine ring exhibit platinum satellites with $^3J(PtH) = 23$ Hz;[15] a full NMR assignment is given in the Experimental Section. The electronic spectrum of the complex appears to be a superposition of ferrocene and $Pt(CH_3)_2(bpy)$, showing a strong metal-to-ligand charge-transfer (MLCT) band at $\lambda_{max} = 516$ nm. Numerous attempts to grow crystals of **2** suitable for structure determination were unsuccessful.

Scheme 2

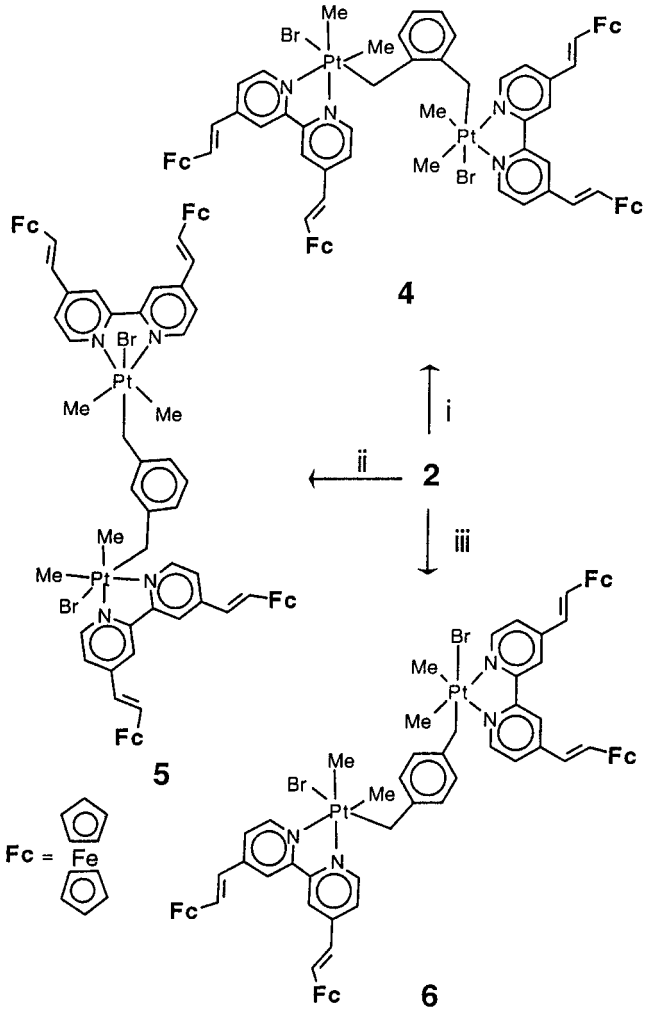

i: *o* - bis(bromomethyl)benzene
ii: *m* - bis(bromomethyl)benzene
ii: *p* -bis(bromomethyl)benzene

Model Compounds. As a model reaction, the oxidative addition reaction of iodomethane to $[PtMe_2(bpy\text{-}Fc_2)]$, **2**, was studied. The reaction proceeded readily in $CHCl_3$ solution at room temperature to yield the oxidative addition product, **3**. The ^{1}H NMR spectrum of **3** shows a singlet at $\delta = 0.68$ ppm with $^2J(PtH) = 74$ Hz for the methyl group trans to the iodine atom; the cis methyl groups gave a singlet at $\delta = 1.51$ ppm with $^2J(PtH) = 70$ Hz. The smaller platinum coupling constants that accompany oxidation of **2** to **3** are characteristic for platinum(II) *vs* platinum(IV) complexes.[15] These features are very helpful in monitoring the oxidative addition reaction and characterizing the products. Generally, the oxidative addition of alkyl halides, RX, to the red solids of the type $[PtMe_2(NN)]$, where (NN) = 2,2′-bipyridine, 1,10-phenanthroline, and related ligands, gives pale yellow solids $[PtXRMe_2(NN)]$.[15] This color change is a result of the much higher energy MLCT band in the platinum(IV) product.

Heteroatomic Organometallic Dendritic Molecules. As expected from the reaction with methyl iodide, complex **2** reacted readily with *ortho-*, *meta-*, *and para*-bis(bromomethyl)-benzene to yield compounds **4**−**6** (Scheme 2). The ^{1}H NMR spectra of these complexes showed no peaks due to $BrCH_2$ groups indicating that the reaction proceeded to completion. In addition, the methyl−platinum coupling constants decreased

(14) Beer, P. D.; Kocian, O.; Mortimer, R. J. *J. Chem. Soc., Dalton. Trans.* **1990**, 3283.

(15) (a) Achar, S.; Scott, J. D.; Vittal, J. J.; Puddephatt, R. J. *Organometallics* **1993**, *12*, 4592. (b) Achar, S.; Scott, J. D.; Puddephatt, R. J. *Organometallics* **1992**, *11*, 2325. (c) Monaghan, P. K.; Puddephatt, R. J. *J. Chem. Soc., Dalton. Trans.* **1988**, 595. (d) Crespo, M.; Puddephatt, R. J. *Organometallics* **1987**, *6*, 2548. (e) Monaghan, P. K.; Puddephatt, R. J. *Organometallics* **1985**, *4*, 1405. (f) Scott, J. D.; Puddephatt, R. J. *Organometallics* **1986**, *5*, 1538. (g) Scott, J. D.; Crespo, M.; Anderson, C. M.; Puddephatt, R. J. *Organometallics* **1987**, *6*, 1772. (h) Levy, C. J.; Vittal, J. J.; Puddephatt, R. J. *Organometallics* **1996**, *15*, 2108. (i) Chaudhury, N.; Puddephatt, R. J. *J. Organomet. Chem.* **1975**, *84*, 105.

Scheme 3

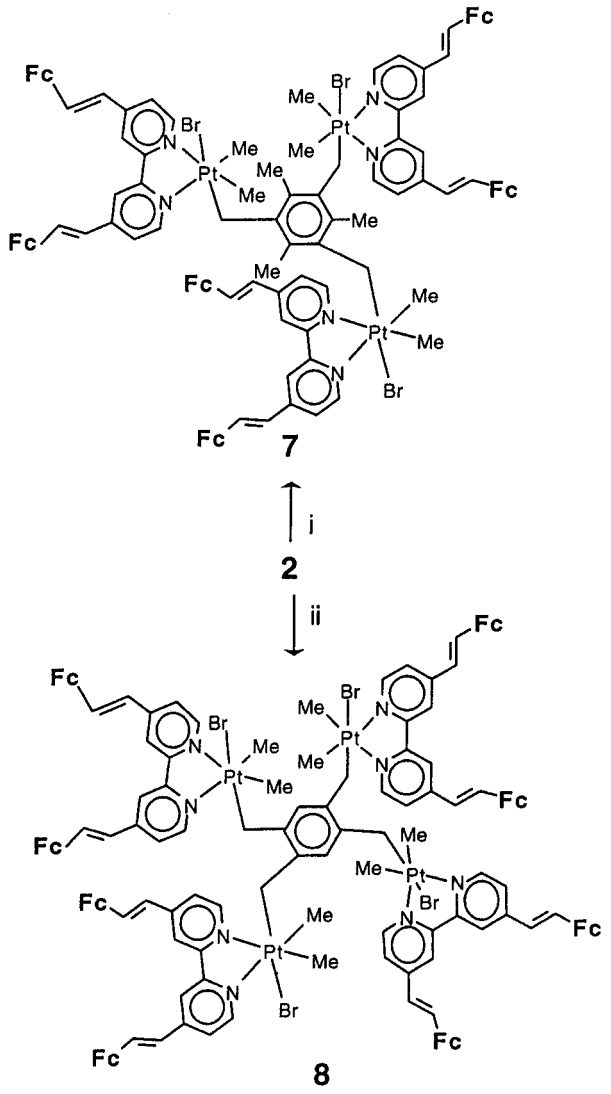

from 86 Hz in **2** to ~70 Hz in **4**−**6**. The CH_2Pt resonance occurred as an AB multiplet, part at $\delta = 1.9-2.3$ ppm and part obscured by the intense solvent resonance at $\delta = 2.5$ ppm. Resonances at $\delta = 6.02$ ppm and 6.2 ppm in **4**, $\delta = 5.88$ ppm in **5,** and $\delta = 5.62$ ppm in **6** are assigned to the central benzene ring protons, which are strongly shielded by the ring current of the bpy-Fc_2 ligands.[4] The resonances in the ^{1}H NMR spectra of **4**−**6** were broader than in **2**, and this may be due to restricted rotation as the molecule becomes congested. All the peaks in the spectrum were assigned, and the details are given in the Experimental Section.

Likewise, the reaction between **2** and 1,3,5-tris(bromomethyl)-mesitylene, 1,2,4,5-tetrakis(bromomethyl)benzene, and 1,2,3,4,5,6-hexakis(bromomethyl)benzene gave compounds **7**−**9**, according to Schemes 3 and 4. In this approach, dendritic arms (each containing one platinum and two ferrocene moieties) are built first and then coupled to a polyfunctional core. The complexes **7**−**9** contain three platinum and six ferrocenyl, four platinum and eight ferrocenyl, and six platinum and twelve ferrocenyl units, respectively. In order to minimize the steric hindrance in **8** and **9**, the adjacent platinum(IV) substituents presumably occupy alternating positions above and below the plane of the central benzene ring. No ^{1}H NMR resonances corresponding $BrCH_2$ groups were observed in the products. In general, the ^{1}H NMR spectra of complexes **7**−**9** showed broad, poorly

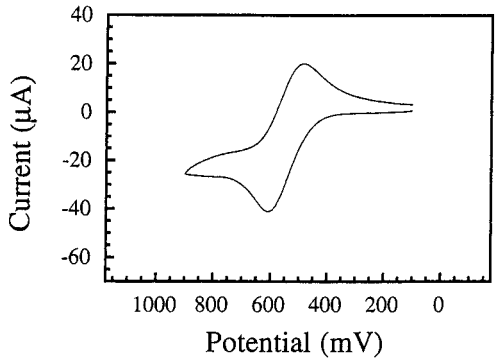

Figure 1. Cyclic voltammogram of **8** in 0.1 *M* $TBA^+PF_6^-/CH_3CN$ at a platinum-disk electrode ($A = 0.031$ cm^2). Scan rate = 0.1 V/s. Potential recorded *vs* AgCl/Ag.

Scheme 4

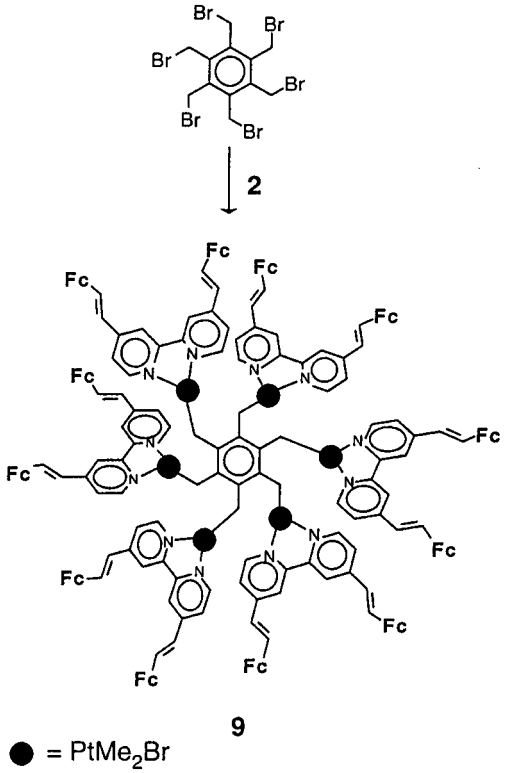

resolved peaks (presumably due to restricted rotation in these congested molecules), but the integration of the spectra, together with the analytical data, supports the proposed formulations. Unfortunately, mass spectrometry failed to yield parent ions, and size-exclusion chromatography could not be performed on these dendritic molecules because of their limited solubility.

Electrochemistry. All of the ferrocene-containing dendritic molecules exhibited reversible multielectron oxidations corresponding to the Fe(III)/Fe(II) couple of the ferrocenyl units.[16] Figure 1 shows the cyclic voltammogram of **8** in 0.1 *M* $TBA^+PF_6^-/CH_3CN$; the appearance of a single oxidation wave at 0.50 V (corresponding to eight electrons as determined by bulk electrolysis) confirms the presence of multiple noninteracting redox sites.[17] Similar CV's and coulometric data were recorded for all model complexes and dendritic molecules.

(16) Upon UV−vis spectroelectrochemical oxidation, the ferrocene-containing species exhibited a strong absorption feature centered at ~650 nm, characteristic of ferrocenium Cp-to-Fe(III) charge transfer: Duggan, D. M.; Hendrickson, D. N. *Inorg. Chem.* **1975**, *14*, 955.

(17) Flanagan, J. B.; Margel, S.; Bard, A. J.; Anson, F. C. *J. Am. Chem. Soc.* **1978**, *100*, 4248.

(18) (a) Christie, J. H.; Anson, F. C.; Lauer, G.; Osteryoung, R. A. *Anal. Chem.* **1963**, *35*, 1979. (b) Rieger, P. H. *Electrochemistry, 2nd ed.*; Chapman & Hall: New York, 1994.

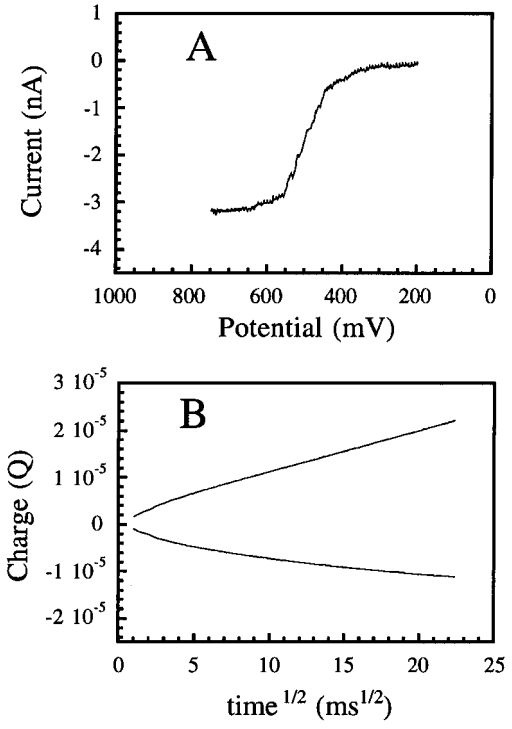

Figure 2. (a) Steady-state voltammogram of **8** in 0.1 *M* $TBA^+ClO_4^-$/DMF at a platinum-disk microelectrode ($d = 30$ μm). (b) Plot of Q *vs* $t^{1/2}$ for **8** recorded during a one-second potential step from 100 to 900 mV at a platinum-disk electrode ($A = 0.031$ cm^2).

These compounds were also studied by a combination of chronocoulometry[18a] and linear-sweep microelectrode voltammetry.[18b] For the chronocoulometric experiment, the diffusional charge is given by eq 1; the corresponding steady-state voltametric current is given by eq 2:

$$Q = \frac{2nFAD^{1/2}Ct^{1/2}}{\pi^{1/2}} \quad (1)$$

$$i_d = 4nFDCd \quad (2)$$

(Here, n is the number of electrons transferred, F is the Faraday constant, A is the area of the electrode, D is the diffusion constant, C is the bulk concentration of analyte in solution, t is the time, and d is the diameter of the microdisk electrode.) Because the slope (S) of the Anson plot (Q *vs* $t^{1/2}$) is proportional to $nD^{1/2}$ while the voltammetric current depends on nD, it is possible to simultaneously calculate n and D from these two experiments, according to eqs 1−3. As the calculated n value

$$D = \left(\frac{i_d A}{2dS\pi^{1/2}}\right)^2 \quad (3)$$

is equal to the number of ferrocenyl repeat units, this method yields the composition of the dendritic materials directly from the transient electrochemical experiments. The advantage of this assay over exhaustive oxidation is that the oxidized species are not required to be stable on the (much longer) bulk-electrolysis time scale. Indeed, for several of the larger dendritic molecules studied here, it was necessary to carry out the electrolyses at low temperature and/or remove the bulk-electrolysis electrode several times during the course of the oxidation to remove passivating films that had formed on the surface.

Figure 2 shows the chronocoulometry and steady-state CV trace for compound **8**. Each dendrimer gave similarly well-behaved responses. All measurements were carried out at relatively low concentrations (≤0.2 mM) to avoid adsorption of the oxidized species to the platinum electrodes. Table 1 summarizes the calculated diffusion constants and n values for compounds **4**−**9**. The excellent agreement between the calculated and known values of n highlights the potential application of simple electrochemical measurements as a means to characterize otherwise intractable dendridic materials.

Table 1. Diffusion Coefficients and n-values for Complexes **4**−**9**

compd	10^6D (cm^2/s)[a]	n(calc)[a]	n(BE)[b]	n(theoret)
4	2.3	3.9	3.7	4
5	2.7	4.1	3.6	4
6	2.6	3.7	3.8	4
7	1.6	5.8	5.7	6
8	1.7	8.3	7.8	8
9	1.1	13.6	11	12

[a] Calculated according to eqs 1−3. [b] Determined by bulk electrolysis.

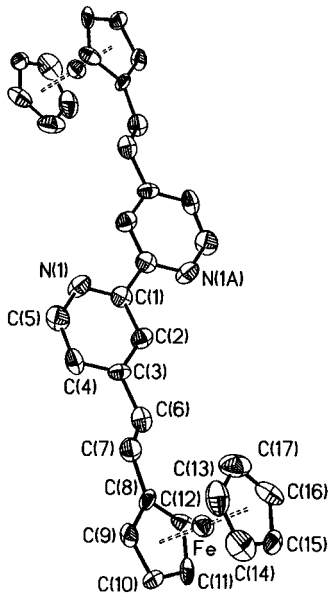

Figure 3. Crystal structure drawing of bpy-Fc_2, **1**, with 40% thermal ellipsoids.

Table 2. Selected Bond Distances (Å) and Angles (deg) for **1**

Fe−C(8)	2.054(11)	Fe−C(9)	2.031(11)
Fe−C(10)	2.039(12)	Fe−C(11)	2.025(11)
Fe−C(12)	2.017(12)	Fe−C(13)	2.017(14)
Fe−C(14)	2.018(13)	Fe−C(15)	2.034(12)
Fe−C(16)	2.018(13)	Fe−C(17)	1.998(13)
C(3)−C(6)	1.491(14)	C(6)−C(7)	1.317(13)
C(7)−C(8)	1.461(14)	Fe···Cp	1.63(1)[a]
Fe···Cp′	1.64(1)[a]		
C(2)−C(3)−C(6)	120.4(12)	C(6)−C(7)−C(8)	128.5(12)
C(4)−C(3)−C(6)	122.9(13)	C(3)−C(6)−C(7)	123.2(12)
C(12)−C(8)−C(7)	127.4(12)		

[a] Cp and Cp′ refer to the centroid of the substituted and unsubstituted cyclopentadienyl moieties, respectively.

X-ray Crystallography. Compound 1. The X-ray structure of compound **1** is shown in Figure 3. The asymmetric unit contains one-half of one bpy-Fc_2 molecule with the other half generated by an inversion. Selected bond distances and angles are given in Table 2, while selected atomic positional parameters are provided in the Supporting Information. The structure is consistent with the solution-state data. The ferrocene moieties are positioned trans to the pyridines, and the pyridine portions lie anti to each other. It is likely that the molecule adopts the anti configuration to remove potential steric interference from H(3) and H(3′). The substituted alkene portion of the molecule is not rigorously planar nor is the pyridine ring coplanar with

Table 3. Selected Bond Distances (Å) and Angles (deg) for **3**

Pt−C(1)	2.05(2)	Pt−C(2)	2.07(2)
Pt−C(3)	2.04(2)	Pt−N(1)	2.175(13)
Pt−N(2)	2.134(12)	Pt−I	2.8021(13)
C(6)−C(9)	1.45(2)	C(9)−C(10)	1.29(2)
C(10)−C(11)	1.45(2)	C(23)−C(26)	1.49(2)
C(26)−C(27)	1.33(2)	C(27)−C(28)	1.43(2)
Fe(1)···Cp	1.66(1)[a]	Fe(1)···Cp′	1.65(1)[a]
Fe(2)···Cp	1.64(1)[a]	Fe(2)···Cp′	1.64(1)[a]

C(1)−Pt−C(2)	90.8(6)	C(1)−Pt−C(3)	84.8(7)
C(2)−Pt−C(3)	87.2(7)	C(1)−Pt−I	176.3(5)
C(3)−Pt−I	92.6(5)	C(2)−Pt−I	91.8(5)
N(1)−Pt−I	85.5(3)	N(2)−Pt−I	90.2(3)
N(2)−Pt−N(1)	78.2(5)	C(1)−Pt−N(1)	92.2(6)
C(1)−Pt−N(2)	92.1(5)	C(2)−Pt−N(1)	174.3(6)
N(2)−Pt−N(1)	78.2(5)	C(2)−Pt−N(2)	96.9(6)
C(3)−Pt−N(1)	97.9(6)	C(3)−Pt−N(2)	175.0(6)
C(6)−C(9)−C(10)	130(2)	C(9)−C(10)−C(11)	126(2)
C(23)−C(26)−C(27)	125.1(14)	C(26)−C(27)−C(28)	126(2)

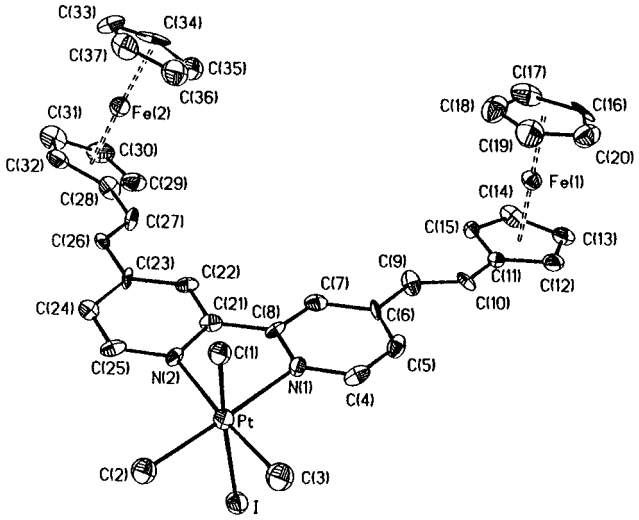

Figure 4. Thermal ellipsoid (40%) drawing of $PtMe_3I(bpy\text{-}Fc_2)$, **3**.

the connected cyclopentadienyl ring. The torsional angle defined by C(3)−C(6)−C(7)−C(8) is 175.4°, while the dihedral angle between the pyridine ring and connected cyclopentadienyl ring is 159.3°. The coordination environment around Fe is typical of ferrocene.[19] The separations between the centroid of the C(8)-containing Cp ring and the C(13)-containing Cp ring are essentially equal at 1.638 and 1.633 Å. The average Fe−C separations for both rings are very close at 2.02 and 2.03 Å for the unsubstituted and subsituted Cp rings, respectively. These can be compared to 2.05Å for ferrocene itself. And, like ferrocene, the conformations of the Cp rings of bpy-Fc_2 are nearly eclipsed with a deviation of only 4° compared to 9° for ferrocene.

Compound 3 ($PtMe_3I(bpy\text{-}Fc_2)\cdot 2CH_2Cl_2$). The asymmetric unit contains the metal complex and two dichloromethane solvates. There are no contacts between these moieties. Selected bond distances and angles are presented in Table 3, while atomic positional parameters are given in the supporting information. The structure of **3** shown in Figure 4 displays a Pt(IV) metal center in a roughly octahedral environment. Most cis angles are within a few degrees of 90° except for the N(1)−Pt−N(2) angle which is contracted to 78.2(5)° as a result of the constrained bite of the bipyridine ligand. As expected, the three methyl groups are arranged in a facial fashion as a result of the trans product from MeI addition. The three Pt−C separations are fairly close to each other at 2.05(2), 2.07(2), and 2.04(2) Å for Pt−C(1), Pt−C(2), and Pt−C(3), respectively.

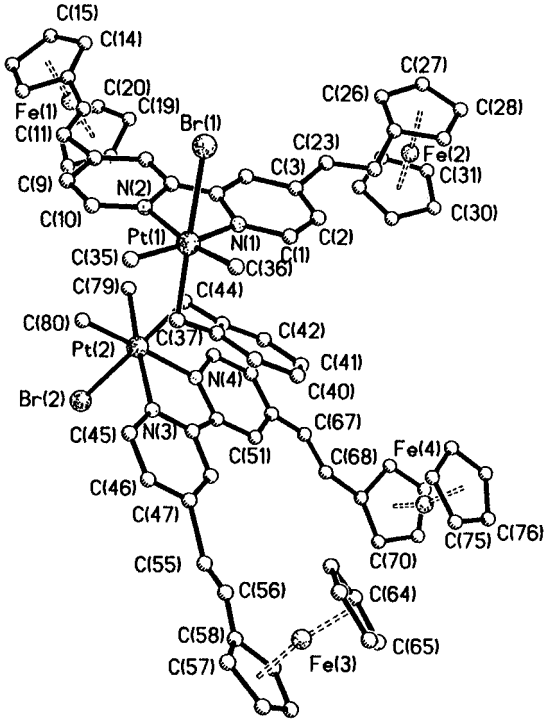

Figure 5. Drawing of partial structure refinement of *o*-{$(CH_2)PtMe_2$-Br(bpy-Fc_2)}$_2C_6H_4$, **4**, with 40% thermal ellipsoids.

The Pt−C separation for the methyl group trans to the I atom is not significantly elongated in spite of the trans influence of I. This may be a result of the uncertainty in this measurement. The Pt−I separation is typical at 2.802(1) Å.

The geometry of the bpy-Fc_2 portion of the molecule is similar to that of the ligand by itself. The ferrocene portions reside on the same side of the ligand and are splayed away from the platinum center. The Fe(1)−Pt and Fe(2)−Pt separations are 10.225 and 10.133 Å.

Partial Structure for Compound 4. Poor quality crystals of **4** were obtained after repeated attempts and modifications by slow diffusion of diethyl ether into a dichloromethane solution of **4**. These deep red cyrstals typically were small stacks of plates and diffracted weakly. However, a partial structure was obtained that clearly shows the ligation and geometry about the Pt centers, the connectivity to the central benzene ring, and the four ferrocene moieties. From Figure 5 it is clear that there are two Pt(IV) centers arranged above and below the plane of the central, ortho-substituted benzene ring as a result of a trans oxidative addition. The location of the heavy atoms can be assigned without question; however, the connectivity through the carbon backbone to the four ferrocene moieties is somewhat distorted because of the low resolution of the structure. The ferrocene portions of the bpy-Fc_2 ligands are arranged with the unsubstituted Cp ring directed towards the central benzene ring and opposite of the bromide ligands. This arrangement likely results from packing considerations. All of the Fc groups are directed towards a void created by the Pt coordination to the central benzene ring. Comments on bond distances and angles of the lighter atoms are not warranted because of the low quality of the data. The coordination environment around the two Pt(IV) centers and their position around the central benzene ring are emphasized in Figure 6.

Conclusions

This paper describes the successful syntheses of a series of novel heteroatomic organometallic dendritic molecules. The reactions occur under mild conditions and in very high yield. Cyclic voltammetry is shown as a powerful tool support the

(19) Seiler, P.; Dunitz, J. D. *Acta Crystallogr.* **1979**, *B35*, 2020.

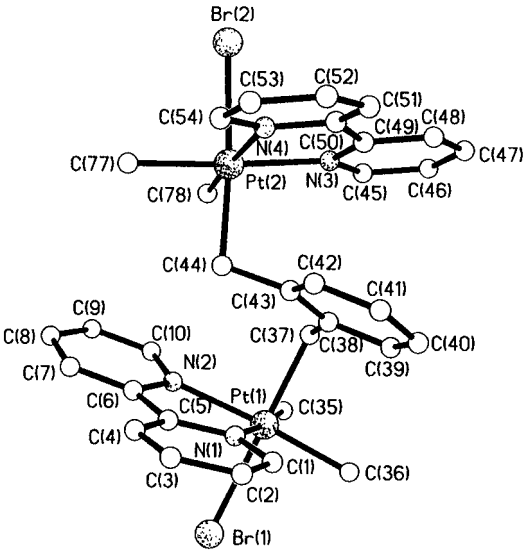

Figure 6. Perspective view of the core of *o*-{$(CH_2)PtMe_2Br(bpy\text{-}Fc_2)\}_2C_6H_4$, **4**.

proposed structures which may prove beneficial in supplementing other methods such as NMR, size-exclusion chromatography, and mass spectrometry.

Experimental Section

The ^{1}H NMR spectra were recorded using a General Electric QE 300 spectrometer. UV−visible spectra were recorded using a Perkin-Elmer lambda 11 spectrometer in 1:1 acetone/benzene solvent. Elemental analyses were performed by Desert Analytics, Tucson, AZ.

All electrochemical experiments were performed using a BAS CV-50W electrochemical analyzer. Cyclic voltammetry (CV) and double potential-step chronocoulometry (CC) were performed at ambient temperature with a normal three-electrode configuration consisting of a platinum-disk working electrode ($A = 0.031$ cm^2), a AgCl/Ag reference electrode, and a platinum-wire auxilliary electrode. Steady-state voltammetric experiments were carried out at a platinum-disk microelectrode ($d = 30$ μm) prepared by encasing a platinum fiber into a uranium-doped glass tip. In each case, the electrode size was determined by measuring the diffusional currents of standardized ferrocene solutions in acetonitrile, assuming a diffusion constant of ferrocene of 2.4×10^{-5} cm^2/s.[20] The working compartment of the electrochemical cell was separated from the reference compartment by a modified Luggin capillary. A large-area platinum-mesh working electode was used for bulk electrolysis experiments. All three compartments contained a 0.1 *M* solution of supporting electrolyte. Acetonitrile (Burdick and Jackson) was distilled from CaH_2 prior to use; dimethylformamide (DMF) (Burdick and Jackson) was vacuum distilled from BaO and 4 Å molecular sieves prior to use. Tetrabutylammonium hexafluorophosphate ($TBA^+PF_6^-$) and tetrabutylammonium perchlorate ($TBA^+ClO_4^-$) were obtained from Southwestern Analytical and used as received.

Potentials are reported *vs* aqueous AgCl/Ag and are not corrected for the junction potential. Under conditions identical with those employed here, the ferrocenium/ferrocene couple[21] has $E^{\circ\prime} = 0.42$ V with $E_{pa} - E_{pc} = 90$ mV. No *iR* compensation was used.

The complex $[Pt_2Me_4(\mu\text{-}SMe_2)_2]$[22] and the ligand 4,4′-bis(ferrocenylvinyl)-2,2′-bipyridine[14] were prepared by literature methods.

Complex 2. This complex was prepared by employing a similar procedure which was used to synthesize [$PtMe_2$(4,4′-di-*tert*-butyl-2,2′-bipyridine)].[15,22] To a stirring solution of the ligand **1** (0.65 g) in benzene (400 mL) was added a solution of $[Pt_2Me_4(\mu\text{-}SMe_2)_2]$ (0.325 g) in benzene (50 mL). The color turned from light pink to burgundy. After being stirred for 0.5 h, the solution was allowed to stand for 1 h. The precipitated product was separated, washed with ether, and dried (0.55 g). The filtrate volume was reduced to nearly 100 mL, and a second crop of the product (0.25 g) was obtained by precipitating with hexane. The compound can be recrystallized from chloroform/diethyl ether. Yield: 88%. Anal. Calcd for $C_{36}H_{34}N_2Fe_2Pt\cdot CHCl_3$: C, 48.3; H, 3.8; N, 3.0. Found: C, 49.3; H, 3.8; N, 3.3. ^{1}H NMR in $CDCl_3$: $\delta = 1.15$ [s, 6H, ^2J(PtH) = 86 Hz, PtMe], 4.16 [s, 10H, C_5H_5 of ferrocene], 4.44 and 4.57 [s, 4H each, C_5H_4 of ferrocene], 6.65 and 7.35 [d, 2H each, =CH, ^3J(HH) = 16 Hz], 7.48 [d, 2H, H^5, H$^{5'}$ of bipyridine, ^3J(HH) = 4 Hz], 7.91 [s, 2H, H^3, H$^{3'}$ of bipyridine], 9.08 [d, 2H, H^6,H$^{6'}$ of bipyridine, ^3J(HH) = 5 Hz, ^3J(PtH) = 23 Hz]. UV−vis: λ_{max}= 516 nm.

Complex 3. To a stirring burgundy colored solution of the complex [$PtMe_2$(bpy-Fc_2)] (0.05 g) in chloroform (50 mL) was added methyl iodide (0.1 mL). After 6 h of stirring, the solvent volume was reduced to nearly 5 mL and hexane (50 mL) was added. The precipitated product was separated, washed with ether, and dried under vacuum. Yield: 80%. Anal. Calcd for $C_{37}H_{37}N_2Fe_2IPt\cdot 0.5\ CHCl_3$: C, 44.9; H, 3.8; N, 2.8. Found: C, 45.7; H, 3.7; N, 3.1. ^{1}H NMR in CD_2Cl_2: $\delta = 0.68$ [s, 3H, ^2J(PtH) = 74 Hz, PtMe trans to I], 1.51 [s, 6H, ^2J(PtH) = 70 Hz, PtMe trans to nitrogens], 4.2 [s, 10H, C_5H_5 of ferrocene], 4.5, 4.63, and 4.75 [s, 4, 2, and 2 H, respectively, C_5H_4 of ferrocene], 6.78 and 7.39 [d, 2H each, =CH, ^3J(HH) = 16 Hz], 7.48 [d, 2H, H^5, H$^{5'}$ of bipyridine, ^3J(HH) = 5 Hz], 8.23 [s, 2H, H^3, H$^{3'}$ of bipyridine], 8.72 [d, 2H, H^6,H$^{6'}$ of bipyridine, ^3J(HH) = 6 Hz, ^3J(PtH) = 18 Hz]. UV−vis: λ_{max}= 508 nm.

Complex 4. To a stirring solution of the complex [$PtMe_2$(bpy-Fc_2)] (0.1 g) in chloroform (100 mL) was added *ortho*-bis(bromomethyl)-benzene (0.016 g) in acetone (25 mL). After 20 h of stirring, the solvent volume was reduced to nearly 5 mL and hexane (50 mL) was added. The precipitated product was separated, washed with ether, and dried under vacuum. Yield: 90%. Anal. Calcd for $C_{80}H_{76}N_4Fe_4Br_2Pt_2\cdot 3CHCl_3$: C, 49.4; H, 4.0; N, 2.82. Found: C, 49.0; H, 3.9; N, 3.1. ^{1}H NMR in dmso-d_6: $\delta = 0.97$ [b, 12H, ^2J(PtH) = 70 Hz, PtMe], 1.9−2.3 [m, 4H, CH_2, partly hidden under solvent peak], 4.20 [s, 20H, C_5H_5 of ferrocene], 4.49 and 4.70 [s, 8H each, C_5H_4 of ferrocene], 6.02 and 6.2 [b, 4H, C_6H_4], 6.55, 6.82, 7.74, 8.5, and 8.8 [unresolved, 20H, =CH and bipyridine]. UV−vis: λ_{max}= 508 nm.

Complex 5. Complex **5** was prepared according to the procedure described above. Yield: 90%. Anal. Calcd for $C_{80}H_{76}N_4Fe_4Br_2Pt_2\cdot 3CHCl_3$: C, 49.4; H, 4.0; N, 2.8. Found: C, 49.4; H, 3.8; N, 2.7. ^{1}H NMR in dmso-d_6: $\delta = 0.97$ [broad, 12H, ^2J(PtH) = 70 Hz, PtMe], 1.9−2.3 [m, 4H, CH_2, partly hidden under solvent peak], 4.20 [s, 20H, C_5H_5 of ferrocene], 4.49 and 4.70 [s, 8H each, C_5H_4 of ferrocene], 5.88 [m, 4H, C_6H_4], 6.55, 6.82, 7.74, 8.5, and 8.8 [unresolved, 20H, =CH and bipyridine]. UV−vis: $\lambda_{max} = 508$ nm.

Complex 6. Complex **6** was prepared according to the procedure described above. Yield: 90%. Anal. Calcd for $C_{80}H_{76}N_4Fe_4Br_2Pt_2$: C, 49.4; H, 4.0; N, 2.8. Found: C, 50.0; H, 3.9; N, 2.8. ^{1}H NMR in dmso-d_6: $\delta = 1.09$ [broad singlet, 12H, ^2J(PtH) = 70 Hz, PtMe], 1.9−2.3 [m, 4H, CH_2, partly hidden under solvent peak], 4.18 [s, 20H, C_5H_5 of ferrocene], 4.48 and 4.66 [s, 8H each, C_5H_4 of ferrocene], 5.62 [m, 4H, C_6H_4], 6.45, 6.82, 7.55, 8.2−8.85 [unresolved, 20H, =CH and bipyridine]. UV−vis: λ_{max}= 508 nm.

The dendritic molecules **7**−**9** were prepared with similar procedures by the reaction of the complex **2** with 1,3,5-tris(bromomethyl)-mesitylene, 1,2,4,5-tetrakis(bromomethyl)benzene, and 1,2,3,4,5,6-hexakis(bromomethyl)benzene in a 3:1, 4:1, and 6:1 molar ratios, respectively.

Complex 7. Yield: 89%. Anal. Calcd for $C_{120}H_{117}N_6Fe_6Br_3Pt_3\cdot 2CHCl_3$: C, 48.2; H, 3.9; N, 2.8. Found: C, 48.9; H, 4.0; N, 2.8. ^{1}H NMR in dmso-d_6: $\delta = 0.8-1.6$ [unresolved, 18H, PtMe], 1.9−2.3 [m, 6H, CH_2, partly hidden under solvent peak], 2.9 [s, 9H, CH_3 of benzene ring], 4.2 [b, shoulder at 4.15, 30H, C_5H_5 of ferrocene], 4.5 and 4.7 [b with shoulders, 12H each, C_5H_4 of ferrocene], 6.3−6.45, 6.6−7.1, 7.4−8.9 [unresolved, 30H, =CH and bipyridine]. UV−vis: $\lambda_{max} = 508$ nm.

Complex 8. Yield: 95%. Anal. Calcd for $C_{154}H_{146}N_8Fe_8Br_4Pt_4\cdot 3CHCl_3$: C, 47.0; H, 3.7; N, 2.8. Found: C, 46.3; H, 3.6; N, 2.7. ^{1}H NMR in dmso-d_6: $\delta = 0.7-1.6$ [unresolved, 24H, PtMe], 2.6−3.0 [m, 8H, CH_2, partly hidden under solvent peak], 4.2 [b, 40H, C_5H_5 of ferrocene], 4.47 and 4.66 [b, 16H each, C_5H_4 of ferrocene], 5.5 [m,

(20) Kuwana, T.; Bublitz, D. E.; Hoh, G. *J. Am. Chem. Soc.* **1960**, *82*, 5811.
(21) Geiger, W. E. *Organometallic Radical Processes;* Trogler, W. C., Ed.; Journal of Organometallic Chemistry Library 22; Elsevier: New York, 1990.
(22) Scott, J. D.; Puddephatt, R. J. *Organometallics* **1983**, *2*, 1643.

Table 4. Crystal Data

compd	**1**	**3**	**4**
formula	$C_{17}H_{14}FeN$	$C_{37}H_{37}Fe_2IN_2Pt\cdot 2CH_2Cl_2$	$C_{80}H_{75}Br_2Fe_4N_4Pt_2\cdot CH_2Cl_2$
fw	288.14	1113.23	1948.75
a, (Å)	11.780(3)	11.497(2)	14.469(12)
b, (Å)	10.662(3)	22.796(6)	15.145(11)
c, (Å)	11.642(3)	15.801(3)	21.33(2)
α (deg)	90	90	69.46(5)
β (deg)	118.61(2)	106.08(1)	71.15(5)
γ (deg)	90	90	81.87(6)
V, (Å^3)	1283.7(6)	3979(2)	4140(6)
space group	$P2_1/c$	$P2_1/n$	$P\bar{1}$
Z	4	4	2
D_{calc} (g/cm^3)	1.491	1.858	1.563
cryst size (mm)	0.40 × 0.02 × 0.05	0.52 × 0.20 × 0.20	0.04 × 0.11 × 0.12
μ(Mo Ka), (mm^{-1})	1.157	5.301	5.120
radiation (λ, Å)	graphite monochromated Mo Kα (0.710 73)	graphite monochromated Mo Kα (0.710 73)	graphite monochromated Mo Kα (0.710 73)
temp (K)	293	193	193
transm factors	0.732−0.778	0.227−0.665	0.847−0.606
R_1,[a] wR_2[b] ($I > 2\sigma(I)$)	0.0625, 0.112	0.0648, 0.1538	0.1244, 0.2825

[a] $R_1 = \Sigma||F_o| - |F_c||/\Sigma|F_o|$. [b] $wR_2 = [\Sigma[w(F_o^2 - F_c^2)^2]/\Sigma[w(Fo^2)^2]]^{0.5}$.

2H, benzene ring protons], 5.8−8.9 [unresolved, 40H, =CH and bipyridine]. UV−vis: λ_{max}= 510 nm.

Complex 9. Yield: 85%. Anal. Calcd for $C_{228}H_{216}N_{12}Fe_{12}Br_6Pt_6\cdot 4CHCl_3$: C, 47.0; H, 3.7; N, 2.8. Found: C, 46.5; H, 3.8; N, 3.0. ^{1}H NMR in dmso-d_6: δ = 0.8−1.7 [unresolved, 24H, PtMe], 1.9−2.3 [unresolved, 12H, CH_2, partly hidden under solvent peak], 4.2 [b, 60H, C_5H_5 of ferrocene], 4.46−4.7 [unresolved, 48H, C_5H_4 of ferrocene], 6.4−7.0, 7.5−8.1, 8.45−8.9 [unresolved, 60H, =CH and bipyridine.

X-ray Data Collection for 4,4′-Bis(ferrocenylvinyl)-2,2′-bipyridine, 1. Red/orange needles of **1** were obtained by the slow diffusion of diethyl ether into a chloroform solution of the complex. A crystal was selected and mounted on a glass fiber with silicone cement and placed on a Siemens P4 diffractometer. Unit cell parameters were determined by least-squares analysis of 19 reflections with 5.45° < 2θ < 19.27°. A total of 1761 reflections were collected between 3.5° < 2θ < 40.0 yielding 1201 unique reflections (R_{int} = 0.0886). The data were corrected for Lorentz and polarization effects. Scattering factors and corrections for anomalous dispersion were taken from a standard source.[23] Crystal data are given in Table 4.

Solution and Structure Refinement for 4,4′-Bis(ferrocenylvinyl)-2,2′-bipyridine, 1. Calculations were performed using Siemens SHELXTL PLUS, version 5.03, system of programs refining on F^2. The structure was solved by direct methods, and there were no unusual features of this refinement. Hydrogen atom positions were calculated using a riding model with a C−H distance fixed at 0.96 Å and a thermal parameter of 1.2 times the host carbon atom. An absorption correction using a semi-empirical model derived from an azimuthal data collection was applied. All non-hydrogen atoms were refined with anisotropic thermal parameters. The largest peak in the final difference map was equivalent to 0.294 e$^-$/Å^3 and was located 1.449 Å from Fe.

X-ray Data Collection for $PtMe_3I(bpy\text{-}Fc_2)\cdot 2CH_2Cl_2$, 3. Deep red plates of **3** were obtained by slow diffusion of diethyl ether into a dichloromethane solution of the complex. A suitable crystal was coated with a light hydrocarbon oil, mounted on a glass fiber, and placed in the −100 °C cold stream of a Siemens P4 diffractometer. Unit cell parameters were determined by least-squares analysis of 23 reflections with 9.96 < 2θ < 25.0. A total of 6683 reflectios were collected were collected between 3.5° < 2θ < 45.0 yielding 5203 unique reflections (R_{int} = 0.0886). Two check reflections showed only random fluctuations in intensity during data collection. The data were treated as described above. The data were corrected for absorption using XABS2.[24]

Solution and Structure Refinement for $PtMe_3I(bpy\text{-}Fc_2)\cdot 2CH_2Cl_2$, 3. The structure was solved and refined as described above. The structure consists of the metal complex and two molecules of dichloromethane. Both solvates suffer from some mild disorder as evidenced by their larger thermal parameters. Models attempting to better describe this disorder lead to poor refinements. Hydrogen atoms were added as described above. All non-hydrogen atoms were refined with anisotropic thermal parameters. The largest peaks in the final difference map was equivalent to 2.43 e$^-$/Å^3 and is located 1.788 Å from Pt.

X-ray Data Analysis for the Partial Structure of *o*-$\{(CH_2)\text{-}PtMe_2Br(bpy\text{-}Fc_2)\}_2C_6H_4\cdot CH_2Cl_2$, 4. Small, thin plates of **4** were obtained by slow diffusion of diethyl ether into a dichloromethane solution of **4.** All of the deep red crystals were partially twinned and diffracted poorly. The best of these crystals was selected and mounted as described for **2**. Unit cell parameters were determined by least-squares analysis of 12 reflections with 5.8 < 2θ < 9.0. A total of 4224 reflections were collected between 3.5° < 2θ < 32.0 yielding 3360 unique reflections (R_{int} = 0.1486). Two check reflections showed only random fluctuations in intensity during data collection. The data were treated as described above.

The structure was solved by direct methods. Because of the poor data quality only the heavy atoms were refined with anisotropic thermal parameters. All of the cyclopentadienyl ligands were idealized as were the bipyridines. Two carbons of the alkene linkages could not be located in any of the Fourier difference maps and were added at calculated positions. Hydrogens were added where appropriate using a riding model described above. An initial absorption correction did not improve the structure and ultimately was not applied.

Acknowledgment is made to the donors of the Petroleum Research Fund, administered by the American Chemical Society, for their support of this research (V.J.C.), to Johnson Matthey for their generous loan of platinum salts (V.J.C.), to the Camille and Henry Dreyfus Foundation (M.G.H.), to The Research Corp. (M.G.H.), and to the NSF (Grant DUE-9551647).

Supporting Information Available: X-ray crystallographic files in CIF format for complexes **1**, **3**, and **4** are available on the Internet only. Access information is given on any current masthead page.

IC961435J

(23) *International Tables for X-ray Crystallography*; Kynoch Press: Birmingham, England, 1974; Vol. 4.
(24) XABS2: Parkin, S. R.; Moezzi, B.; Hope, H. *J. Appl. Crystallogr.*, **1995**, *28*, 53.